Available online at www.sciencedirect.com
SCIENCE DIRECT®
Journal of Catalysis 225 (2004) 170–178
JOURNAL OF CATALYSIS
www.elsevier.com/locate/jcat

Coverage of palladium by silicon oxide during reduction in H_2 and complete oxidation of methane

Guanghui Zhu,[a] Ken-ichiro Fujimoto,[b] Dmitri Yu. Zemlyanov,[a] Abhaya K. Datye,[c] and Fabio H. Ribeiro [a,*]

[a] *Worcester Polytechnic Institute, Department of Chemical Engineering, Worcester, MA 01609-2280, USA*
[b] *Energy & Environment Research Lab., Advanced Technology Research Laboratories, Nippon Steel Corp., 20-1 Shintomi, Futtsu 293-8511, Japan*
[c] *Center for Microengineered Materials, University of New Mexico, Albuquerque, NM 87131, USA*

Received 12 December 2003; revised 22 March 2004; accepted 24 March 2004

Available online 12 May 2004

Abstract

The interaction between silica and palladium following complete oxidation of methane or following reduction in H_2 was investigated on a polycrystalline palladium foil and on supported Pd/SiO_2 catalysts. During methane oxidation, oxidized silicon covered the palladium oxide surface as observed by TEM on Pd/SiO_2 catalysts and by XPS on palladium foil. On the Pd foil, the source of silica was a silicon impurity, common on bulk metal samples. The migration of oxidized silicon onto PdO deactivated the catalysts by blocking the active sites for methane oxidation. Silicon oxide overlayers were also observed covering the Pd surface after reduction of Pd/SiO_2 by H_2 at 923 K.

Keywords: Complete methane oxidation on palladium; Deactivation of Pd by silica; Model catalysts

1. Introduction

Catalytic methane combustion is an environmentally benign process for power generation because of its potential to generate NO_x emissions below 1 ppm; it can also be utilized to remove residual methane in the emission gases in vehicles powered by natural gas. The catalyst in methane combustion must be resistant to deactivation caused, for example, by interaction with the support and substrate materials and contaminants by airborne dust [1]. Since palladium-based catalysts are the most effective catalysts for methane oxidation and silica (SiO_2) is a common support, a major component of air dust and a common contaminant in catalyst supports, it is of practical importance to understand the interaction between palladium and silica during catalytic methane oxidation. In addition, since silicon is a common impurity in bulk Pd and it is difficult to analyze without surface science techniques, results in the literature that use Pd as a foil or wire must be interpreted carefully.

The interaction between the catalytic active metal and an oxide has been growing in importance in catalysis. Virtually all nanoparticle catalysts are dispersed on supports to mitigate particle sintering. Metal–oxide interaction is inherent in these catalysts [2] and may be a potential control variable. A new dimension was added to this possibility with the discovery of the strong metal–support interaction (SMSI) [3,4] manifested by the loss of chemisorption capacity when Pt on titania was reduced in H_2 at about 800 K. It was later found that this effect was caused by titanium suboxide decorating and thus blocking the surface of the Pt particles. More details are contained in the review by Haller and Resasco [5]. A substantial catalytic enhancement effect was found when a reducible oxide interacted with a group VIII metal, but only for certain reactions. Resolution of these initially surprising results showed the importance of surface thermodynamics in determining wetting of the metal by the oxide and ways that bonding at metal–oxide adlayer interfaces or perturbations of the metal chemistry by proximity of the oxide phases could affect catalysis [5–9].

In this contribution, we will be concerned in particular about the interactions between silica and Pd or PdO catalysts supported on silica and its effect on catalytic behavior. Sim-

* Corresponding author. Current address: School of Chemical Engineering, Purdue University, 480 Stadium Mall Drive, West Lafayette, IN 47907-2100, USA.
E-mail address: fabio@purdue.edu (F.H. Ribeiro).

0021-9517/$ – see front matter
doi:10.1016/j.jcat.2004.03.033

ilar effects on other metals and oxides have been reported before [10–23]. Reduction of Pd/SiO_2 in H_2 at a temperature above 723 K could form palladium silicides, such as Pd_2Si [10], Pd_3Si [11,12,21], Pd_4Si [12,21], with the type of silicide formed depending on the reduction conditions. The interaction between Pd and silica was responsible for the selectivity enhancement on the isomerization of neopentane [11]. Another example is the low-temperature reduction of Pd/SiO_2 at 573 K by H_2, which created amorphous silica overlayers on the surface of palladium particles, presumably by silica migration [13]. Not only can H_2 facilitate the interaction between silica and metal or metal oxide, but also water. Silica migration was observed on an iron oxide/silica model catalyst at 670 K on treatment in H_2O/CO or H_2O/H_2 gas mixture, but was not observed on treatment in CO_2/CO or O_2 [14]. After treating a silica-supported magnetite catalyst in a water-containing environment at 650 K and near-atmospheric pressure, the apparent turnover rate for water–gas shift was reduced by approximately one order of magnitude, although the capacity to chemisorb NO did not diminish significantly [15,16]. Muto et al. [17,18] tested Pd/SiO_2, Pd/Al_2O_3, and Pd/SiO_2–Al_2O_3 catalysts for methane oxidation. Their results showed that when the amount of silica on the surface of the support was enough to cover the entire surface of the catalyst, only deactivation was observed during reaction; otherwise activation followed by deactivation was observed. Deactivation of silica-supported cobalt catalysts was observed during Fischer–Tropsch synthesis. It was caused by a loss of active sites and BET surface area [19]. The deactivation increased with water partial pressure. Cobalt–silicate formation and support breakdown, caused by the reaction product water, were proposed as the reasons for deactivation.

The objective of this contribution was to investigate the effect of silica on palladium catalysts during complete oxidation of methane and reduction in H_2. The investigations were carried out on model catalysts consisting of polycrystalline palladium foil and palladium supported on nonporous silica. Palladium supported on ZrO_2, a more inert support, was also studied to allow for a better understanding of the interaction between silica and palladium. The advantages of these catalysts are that they can be easily examined by surface-sensitive techniques and by TEM [24], respectively. We conclude that silica poisons the catalyst by spreading and covering the surface of PdO in the presence of water at reaction temperature or during H_2 reduction.

2. Experimental methods

2.1. Supported model catalysts

Two supported model catalysts, palladium supported on zirconia (Pd/ZrO_2) and palladium supported on silica (Pd/SiO_2), were studied for methane combustion. The silica support was prepared using the technique developed by Stoeber et al. [25]. By varying the reactant concentrations, monodisperse silica spheres were produced with average diameters between 100 and 500 nm. The material was nonporous and had a simple spherical geometry. The palladium was supported on the silica spheres by nonaqueous impregnation from Pd acetylacetonate (Aldrich) precursor followed by drying in air at room temperature. Palladium supported on zirconia was prepared by incipient wetness impregnation of zirconia (RC-100P, Daiichi Kigenso Kagaku Co., 16.5 $m^2\,g^{-1}$, air treatment at 1123 K, 10 h) with $Pd(NH_3)_2(NO_2)_2/HNO_3$ solutions (Tanaka Kikinzoku Kogyo Co.) and then dried in air at 373 K for 24 h.

The number of exposed Pd atoms was measured using H_2–O_2 titration after samples were reduced in H_2 (2–4 $cm^3\,H_2\,g^{-1}\,s^{-1}$) at 373 K for 1 h and evacuated at 373 K for 1 h to remove chemisorbed hydrogen. The uptake of O_2 during O_2 chemisorption and of H_2 during titration of chemisorbed oxygen by H_2 was measured at 373 K and 2.7–11 kPa H_2 or O_2. Monolayer values were obtained by extrapolating isotherms to zero pressure. The number of exposed Pd metal atoms was calculated using reported stoichiometries [26]:

$$\mathrm{Pd} + \tfrac{1}{2}\mathrm{O_2} \rightarrow \mathrm{PdO} \quad (\mathrm{O_2\ chemisorption}),$$
$$\mathrm{PdO} + \tfrac{3}{2}\mathrm{H_2} \rightarrow \mathrm{PdH} + \mathrm{H_2O} \quad (\text{titration of adsorbed oxygen by } \mathrm{H_2}).$$

Crystallite sizes were estimated from these dispersions by assuming hemispherical crystallites and a Pd surface density of $1.27 \times 10^{19}\ m^{-2}$ [27], which corresponds to the average density on the (111), (100), and (110) planes.

The surface morphology of the supported model catalysts was examined by a Jeol 2000-FX transmission electron microscope. The reaction rate was measured in a tubular reactor with a thin layer of catalyst held above acid-washed quartz wool. This design achieved low methane conversion in a single pass, which made it possible to calculate the turnover rate (number of CO_2 molecules formed per Pd on the surface per unit of time) by assuming differential reactor behavior. The reaction was carried out at 553 K and atmospheric pressure with reactant composition of 2% CH_4, 20% O_2, and 78% He.

2.2. Foil catalyst

The palladium foil catalyst was a 0.125-mm-thick polycrystalline foil (Goodfellow, 99.99+%) with a geometric area of $\sim 1.0\ cm^2$. Methods to mount the catalyst were described previously [28].

Methane oxidation on palladium foil was performed in a batch reactor, which was attached to an ultrahigh vacuum (UHV) chamber equipped with surface analysis tools. Without exposure to the atmosphere, the foil could be transferred between the reactor and the UHV chamber by a welded bellows transfer arm. The batch reactor had a volume of about 0.84 L. A gas pump (Metal Bellows Model MB-21) was used to mix the gases. To carry out the reaction, the foil was transferred to the reactor cell from the UHV chamber and

then the reactants were introduced into the reactor individually. The gas mixture was circulated in the reactor by the gas pump at a nominal rate of 5000 $cm^3\,min^{-1}$ for 25 min before the reaction was started. Gas-phase concentration was monitored by an Agilent 6890 Series gas chromatograph equipped with a 15-ft Carboxen 1000, 60/80-mesh column, and a thermal conductivity detector (TCD). X-ray photoelectron spectroscopy (XPS) and temperature-programmed desorption (TPD) were employed to characterize the foil surface. In the water treatment experiment, water was added by evaporation from the degassed liquid. Blank experiments on a stainless-steel foil revealed that the turnover rate was negligible compared to the turnover rate on the palladium foil [28].

XPS spectra were collected using Al-K_α (1486.6 eV) radiation at 300 W. The atomic sensitivity factor (ASF) used for surface composition calculation from XPS spectra were 0.27 for Si 2s, 0.66 for O 1s, and 4.6 for Pd 3d [29]. The relative atomic concentration for silicon was calculated by

$$\text{nominal atomic concentration of Si} = \frac{\frac{I_{\mathrm{Si2s}}}{\mathrm{ASF}_{\mathrm{Si2s}}}}{\frac{I_{\mathrm{Si2s}}}{\mathrm{ASF}_{\mathrm{Si2s}}} + \frac{I_{\mathrm{Pd3d}}}{\mathrm{ASF}_{\mathrm{Pd3d}}} + \frac{I_{\mathrm{O1s}}}{\mathrm{ASF}_{\mathrm{O1s}}}} \times 100\%,$$

where, for example, I_{Pd3d} is the signal intensity of Pd 3d.

The foil-cleaning procedure consisted of sputtering with a 2 keV Ar ion beam, followed by annealing at 873 K for 1 min under UHV conditions. For the clean foil, only metal palladium features were observed by XPS. Depth profiling of the deactivated foil consisted of cycles of sputtering with 500 eV Ar and XPS analysis.

Temperature-programmed desorption was carried out in the UHV chamber by heating the foil from room temperature to 873 K at 3 $K\,s^{-1}$. Species desorbed from the surface were examined by an UTI-100C quadrupole mass spectrometer.

3. Results

3.1. Surface characterization before reaction

3.1.1. Supported model catalysts

Before reaction, each supported model catalyst was either reduced in H_2 at 923 K for 2 h or oxidized in O_2 at 923 K for 2 h. The specific surface area of treated catalysts is listed in Table 1. Oxidized Pd/ZrO_2 has 1.5 times the specific Pd surface area of the reduced Pd/ZrO_2; oxidized Pd/SiO_2 has 3 times the specific surface area of the reduced Pd/SiO_2. The turnover rate and rate of reaction per gram of Pd after 24 h on stream are also shown in Table 1. The turnover rate for the sample supported on zirconia after reduction and oxidation is about the same, whereas the turnover rate for the Pd catalyst supported on silica is 15 times lower after reduction than for the sample after oxidation. This result shows a significant difference in rate between the samples supported on silica and zirconia and for this reason they were further investigated by TEM. Comparison with rates from the literature is also presented in Table 1 [28,30,31].

The Pd samples supported on zirconia show the expected particle size and features after reduction (Fig. 1) and oxidation (Fig. 2). The same observation is true for the oxidized Pd/SiO_2 (Fig. 3). However, on the reduced Pd/SiO_2 sample amorphous overlayers covering the palladium particles were observed by TEM (Fig. 4). The surface overlayers look amorphous, which is consistent with the migration of silica over the Pd metal surface. It is not possible to estimate the surface coverage of silica since TEM provides a 2D image of a 3D sample; only the silica overlayer at the edge is visible. Since these are randomly oriented particles, one would expect the presence of silica on the top and bottom of the metal particle, which is not visible because the lattice image dominates the contrast. Based on the thickness of the layer, we can state that the coverage is less than one full monolayer.

Table 1
Surface area and corrected turnover rates for Pd catalysts

Catalyst	Pds[a] ($\mu mol\,g^{-1}$)	Diameter[b] (nm)	Rate[c,d] ($\mu mol\,g^{-1}\,s^{-1}$)	TOR[d,e] ($10^{-2}\,s^{-1}$)	Reference
5% Pd/SiO_2-reduced	11	45	1.6	0.7	This work
5% Pd/SiO_2-oxidized	33	15	72	11	This work
10% Pd/ZrO_2-reduced	43	20	37	9	This work
10% Pd/ZrO_2-oxidized	65	15	71	11	This work
10% Pd/ZrO_2	32	30	0.7	3	[30]
1.0% Pd/ZrO_2	2.4–21	4.6–39	0.05–2.1	0.5–11	[31]
Pd foil	–	–	–	70	[28]
Pd black	990[f]	–	–	6	[28]

[a] Pd surface area measured by H_2–O_2 titration at 373 K on fresh catalysts.
[b] Calculated using $d(\mathrm{nm}) = 100/(\text{percentage of metal exposed})$.
[c] Reaction rate based on mass of Pd.
[d] Rate and turnover rate (TOR) calculated at 553 K, 16 Torr CH_4, and 1 Torr H_2O by assuming reaction order of 1 for CH_4, −1 for H_2O, and 0 for O_2 and CO_2.
[e] Turnover rate was calculated based on the surface area measured on fresh catalysts.
[f] Calculated based on BET surface area 47 $m^2\,g^{-1}$.

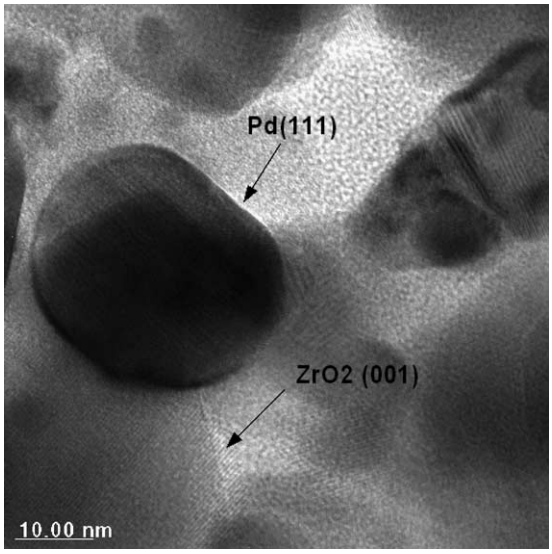

Fig. 1. TEM of Pd/ZrO_2 after reduction in H_2 at 923 K for 2 h.

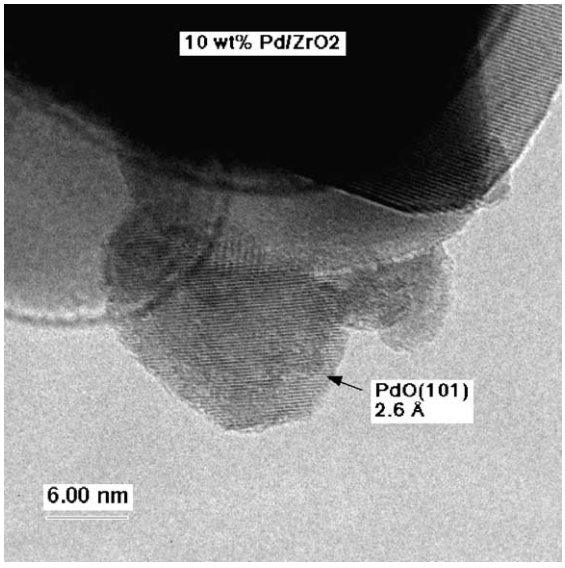

Fig. 2. TEM of Pd/ZrO_2 after oxidation in O_2 at 923 K for 2 h.

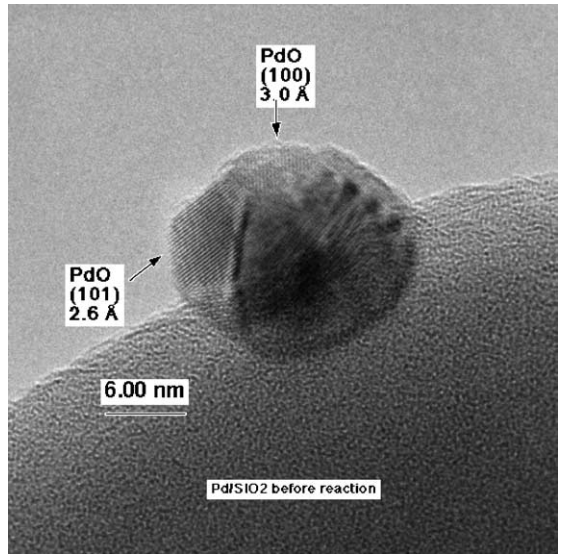

Fig. 3. TEM of Pd/SiO_2 after oxidation in O_2 at 923 K for 2 h.

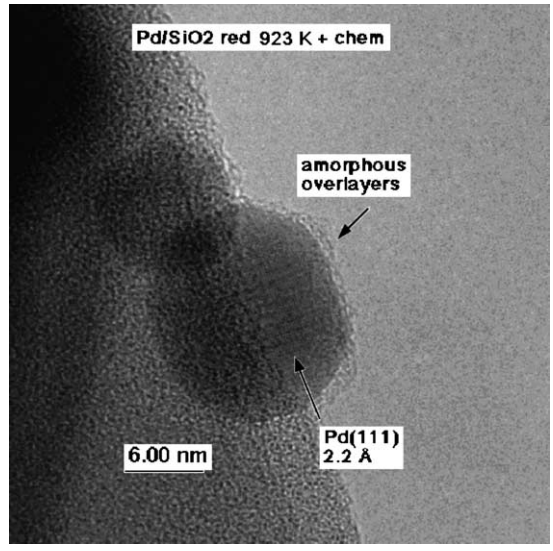

Fig. 4. TEM of Pd/SiO_2 (reduced in H_2 at 923 K for 2 h) after chemisorption. Note amorphous silica overlayers.

3.1.2. Pd foil

Before reaction, the palladium foil was cleaned as described above and then examined by XPS, showing only palladium in the metallic state. Palladium metal was characterized by a Pd $3d_{5/2}$ peak with binding energy (BE) of 334.5 eV. XPS sensitivity toward Si was estimated to be 1%. The number of active sites during methane oxidation was calculated based on a Pd atom density of 1.27×10^{19} m^{-2} [27].

3.2. Surface coverage by silicon compounds during reaction

3.2.1. Supported model catalysts

All Pd/ZrO_2 catalysts showed activation and deactivation stages during reaction, independently of prereduction or preoxidation treatment (Fig. 5). Activation and deactivation stages were also observed for reduced Pd/SiO_2; but only deactivation was observed for oxidized Pd/SiO_2 (Fig. 6). After 24 h on stream, the reduced catalysts generally had lower turnover rates than the oxidized ones. In particular, the turnover rate for the reduced Pd/SiO_2 was 1/15 of the one for oxidized Pd/SiO_2. Oxidized Pd/SiO_2 was examined by TEM after reaction and its image showed that the palladium particles were covered with an amorphous layer (Fig. 7). This amorphous layer was less distinct than the one observed after reduction at 923 K (Fig. 4).

3.2.2. Foil catalyst

A batch reactor was used for measuring rates. Before the results are presented, we will explain how to interpret

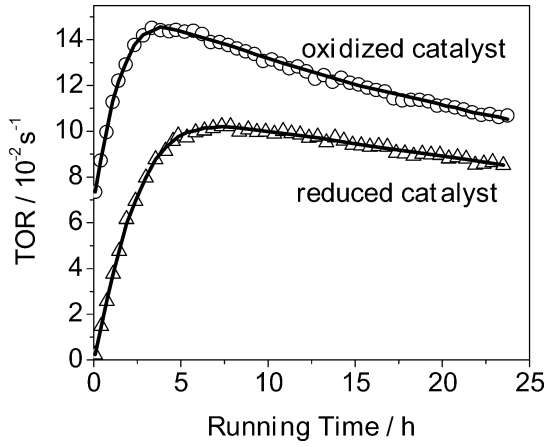

Fig. 5. Turnover rates as function of time for 10% Pd/ZrO_2 (calculated at 553 K, 16 Torr CH_4, 160 Torr O_2, and 1 Torr H_2O using reaction orders 1 for CH_4, −1 for H_2O and 0 for O_2).

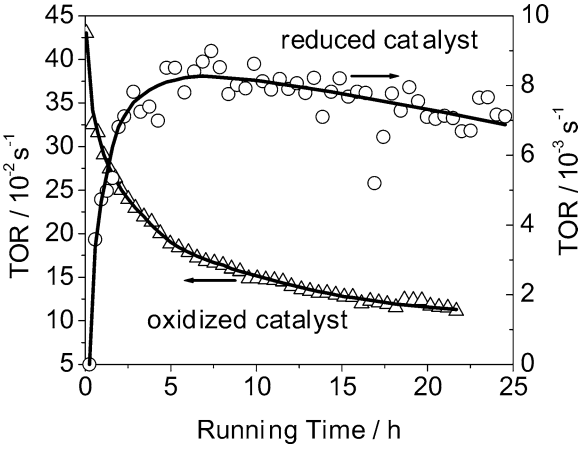

Fig. 6. Turnover rates as function of time for 5% Pd/SiO_2 (calculated at 553 K, 16 Torr CH_4, 160 Torr O_2, and 1 Torr H_2O using reaction orders 1 for CH_4, −1 for H_2O and 0 for O_2).

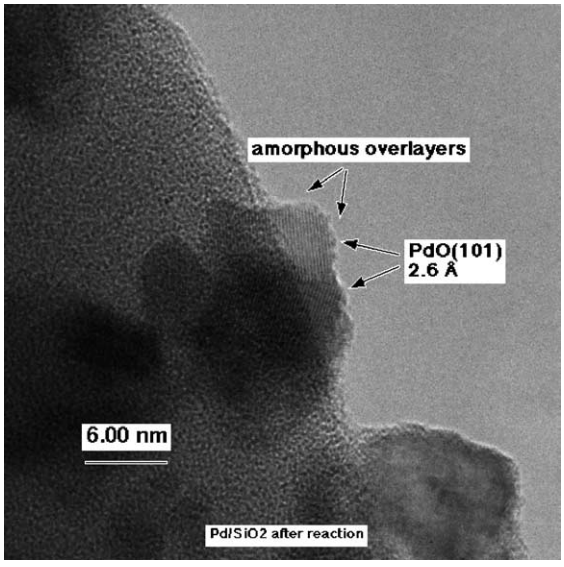

Fig. 7. TEM of oxidized Pd/SiO_2 after methane oxidation reaction at 553 K for 22 h with 2% CH_4, 20% O_2, and N_2 balance to 800 Torr.

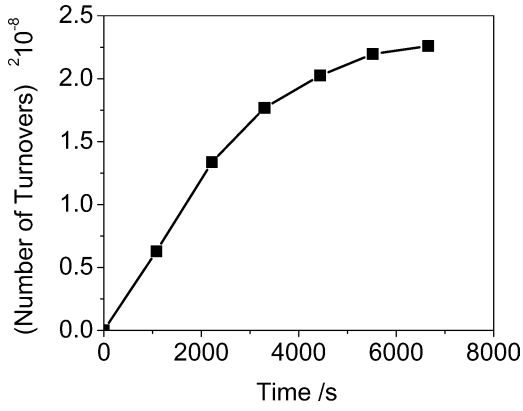

Fig. 8. (Number of turnovers)^2 as function of reaction time for a deactivated foil. Reaction at 598 K with 2% CH_4, 20% O_2, and N_2 balance to 800 Torr.

the data on this type of reactor when inhibition by one of the products is present. For lean fuel methane combustion at 598 K, the methane reaction rate can be expressed as $r = -k[CH_4]^1[O_2]^0[H_2O]^{-1}[CO_2]^0$. At low conversion, the methane concentration is almost constant and the rate expression can be simplified as $r = A/[H_2O]$, where A is a constant. Since the reaction rate was measured in a batch reactor, the water concentration can be related to the change of methane concentration $[H_2O] = 2[CH_4]_0\tau$, where $[CH_4]_0$ is the initial methane concentration and τ is methane conversion. The final expression can be written as $r = B/\tau$, where B is a constant. The reaction rate can also be expressed by methane consumption rate as $-V[CH_4]_0\, d\tau/dt$, where V is the reactor volume and t is reaction time. By combining the two rate expressions, $d\tau/dt = C/\tau$, where C is a constant. After integration, a linear relation can be obtained between the square of conversion and time ($\tau^2 = 2Ct$). Since a relation between methane conversion and number of methane turnovers can be expressed as (number of turnovers) $= D\tau$, where D is a constant, a linear relation can be obtained between (number of turnovers)^2 and reaction time as (number of turnovers)$^2 = Et$, where E equals $2D^2C$. Monteiro et al. [28] reported a linear relationship between (number of turnovers)^2 and reaction time for palladium foil. In this study, the plot of (number of turnovers)^2 to reaction time was used to monitor catalyst performance.

Fig. 8 shows the plot of (number of turnovers)^2 versus reaction time for a typical deactivation process. Since a stable foil produces a straight line, a change in slope indicates deactivation. On the deactivated foil, palladium, oxygen, silicon (Fig. 9), and carbon were observed on the surface. Carbon on the surface was mainly deposited during transfer from the reactor to the UHV chamber. For this reason, carbon was not considered during surface composition analysis. Palladium $3d_{5/2}$ binding energy shifted to 336.3 eV, characteristic of PdO. The Si 2s peak is quite broad and centered at 152.5 eV. According to literature data, the Si 2s peak position for silicon is 150.5–150.7 eV [32–34]. Therefore, the 2 eV shift toward higher BE points to oxidized silicon after reaction. On the other hand, silica (SiO_2) is characterized by the Si 2s

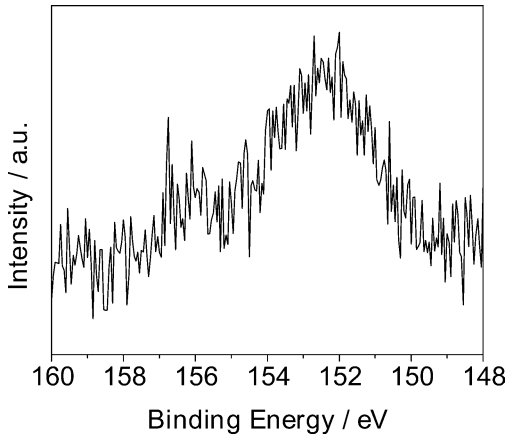

Fig. 9. Si 2s core-level XPS spectra of deactivated foil.

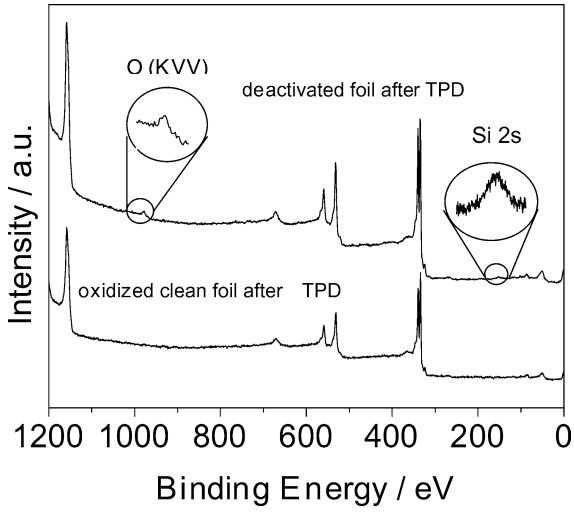

Fig. 10. XPS survey spectra of (a) deactivated foil after TPD (b) oxidized clean palladium foil after TPD.

peak set at approximately 154.2–154.8 eV [35–38]. The factors which cause this smaller BE shift will be treated in the discussion section.

To understand how Si appeared on the surface, a series of experiments were carried out on the clean foil to investigate the effect of H_2O and O_2. The joint effect from H_2O and O_2 was tested by treating the clean foil at 598 K for 30 min with a gas mixture of 2 Torr H_2O, 638 Torr N_2, and 160 Torr O_2. XPS analysis on this foil showed features corresponding to Pd, O, Si, and C. The rate of methane oxidation on the treated foil was tested at 598 K; no CO_2 was detected at 40 min, indicating that the foil was deactivated. After the methane oxidation experiment, the foil was transferred to the UHV chamber and annealed at 873 K for 1 min. XPS analysis of the sample revealed O and Si (Fig. 10), also metallic Pd, on the surface. The nominal atomic concentration assuming a uniformly distributed concentration over the probing volume was 5.2% Si, 16.3% O, and 78.5% Pd.

The O_2 effect on Si was tested by treating the clean foil with 160 Torr O_2 at 598 K for 1 h. No Si was detected by

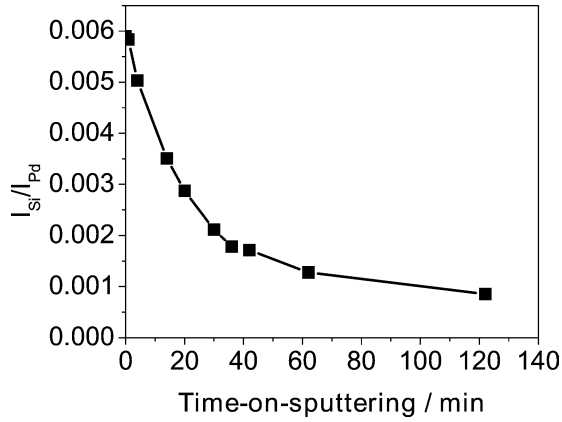

Fig. 11. I_{Si}/I_{Pd} change as function of time-on-sputtering (I_{Si}, XPS signal intensity of Si 2s; I_{Pd}, XPS signal intensity of Pd 3d).

XPS on the oxidized foil. XPS after TPD showed metallic Pd peaks, but did not show O Auger peaks and Si 2s peak (Fig. 10).

The water effect on Si was tested by treating the clean foil with a gas mixture of 3 Torr H_2O and N_2 balance to 800 Torr for 1 h at either room temperature or 598 K. Silicon was detected by XPS on the foil treated at 598 K, but was not detected on the one treated at room temperature.

The information depth of XPS is in the range of 5–10 nm; therefore, additional experiments were performed to determine the depth profile of the Si distribution (Fig. 11). The deactivated catalyst was sputtered by a 0.5 kV Ar^+ beam with beam current of 0.24 μA. The surface composition was analyzed by XPS during sputtering. It can be seen that the signal intensity ratio of silicon to palladium (I_{Si}/I_{Pd}) decreased with sputtering time, pointing to a surface covered by silicon, as discussed in more detail below.

4. Discussion

4.1. Deactivation by coverage with silicon oxides

Silicon and carbon were two impurities found on the surface of the deactivated foil. Previous work [28] showed that carbon does not deactivate the catalyst; thus silica is responsible for deactivation of the foil. One possible source of silica was the bulk of the foil. If conditions are favorable, silicon compounds can migrate to the surface and then agglomerate to form large particles. Our hypothesis is that these large particles, with low concentration and small surface area to volume, generate a low intensity XPS signal that could not be detected on the clean foil. These particles are probably concentrated at grain boundaries. At reaction temperature (598 K) and with help from water formed during reaction, silicon from the large particles could oxidize, spread, and cover the foil. The silica coverage in this case is high and XPS could detect it. The cleaning process could only remove thin layers of silica spreading on the surface, but could not eliminate the large particles that are the source of silica.

Silicon and oxygen were observed on the surface of the deactivated foil after annealing at 873 K (Fig. 10). This oxygen species is associated with Si because PdO decomposes to Pd upon heating in UHV. No oxygen signal is observed by XPS following annealing of a foil that did not show deactivation during reaction (Fig. 10). Bader et al. [39] observed that thermal decomposition of PdO to 1173 K could not decompose the coexisting Si-stabilized oxide. Thus, annealing at 873 K could leave Si-stabilized oxide on the foil surface. Two kinds of oxidized silicon, including silica (SiO_2) and silicon monoxide (SiO), could be the species on the surface [40]. Solid SiO is a metastable state, thermodynamically stable only as a gas at high temperatures; it dissociates to Si and SiO_2 at 400–700 °C [40]. The binding energy of the Si 2s peak was 152.5 eV. This value is approximately 2 eV higher than the one for silicon [32–34]. On the other hand, this BE is lower by approximately 2 eV than the BE characteristic of SiO_2 (154.2–154.8 eV) [35–38]. The relatively small chemical shift might be due to the "surface" nature of the silica. The silica layer covering the surface might consist of silicon atoms bound to various oxygen atoms. Bekkay et al. [41] reported nonstoichiometric oxide formation and the silicon atoms coordinated to one and four oxygen atoms were characterized by the Si 2s peaks at 150.2 and 153.9 eV, respectively. In our case the Si 2s peak is broad and the state of Si could not be unambiguously identified because the signal to noise level on the Si 2s peak was low.

The other factor which might cause the relatively low BE of the Si 2s peak observed in our experiments is the relaxation energy. The variation of the relaxation energy is the final-state effect corresponding to a reorganization of the electrons of the neighboring atoms that provide the screening of the photoelectron hole remaining after electron emission. The effects of relaxation could cause a low BE shift whereas the effect of initial states for a positive ionic state should result in a high BE shift. For example, a large extra-atomic relaxation energy contribution for CdO reduces the BE [42]. Silver is another example of the exceptions which show a low BE shift in the oxide state [42–45]. Therefore, the relatively low BE shift of the Si 2s peak observed in our experiments might be governed by the difference in the relaxation energy. As a rule of thumb, larger relaxation energies are expected for a bulk material as compared to a thin layer or small particles in the 10 nm size range. However, because we have a nonhomogeneous distribution of thin SiO_2 film supported on PdO, the palladium oxide might contribute to the relaxation energy and the resulting value of the thin SiO_2 film might be higher than the corresponding value for bulk SiO_2. Thus, we believe the silicon compound on the surface was silica.

XPS depth profiling indicates that silica was on the top layer of the foil surface. By using Ar^+ with 500 eV ion energy, the sputtering yields for single-element solids are 0.5 Si atom per Ar^+ and 2 Pd atoms per Ar^+ [46]. If Pd were surface segregated compared to Si or the distribution of Pd and Si was homogeneous, then I_{Si}/I_{Pd} should have increased with time-on-sputtering because Pd has a higher sputtering yield. This hypothesis does not agree with the experimental results. The only reasonable element distribution to explain the data is that Si was surface segregated so that I_{Si}/I_{Pd} could drop from the beginning of sputtering even though Si has a lower sputtering yield than Pd.

Assuming silica spreading on top of PdO, the Si 2s and Pd 3d signal intensity could be expressed as a function of silica coverage using a mathematical model for photoelectron attenuation during XPS analysis [47]. The coverage on the deactivated foil was obtained by fitting the signal intensities from the experiment to the mathematical model. The inelastic-mean-free path was obtained from the National Institute of Standards and Technology [48]. The thickness of one monolayer of silica was estimated at 0.34 nm. It was calculated based on the parameters for quartz using the equation $1000\rho a^3 N = A$ where ρ is the quartz density ($\mathrm{kg\,m^{-3}}$), "a" is the monolayer thickness we are estimating, N is the Avogadro number, and A is the atomic weight. The XPS data were recorded with a fixed emission angle of the photoelectron, which was between 0 and 45 ° with respect to the sample normal. With these assumptions, the coverage was found to be in the range of 0.8 to 1.0 monolayer.

Our experimental results showed that water and reaction temperature were the two key factors promoting silica migration, which was in agreement with previous work. Lund and Dumesic [14] observed silica migration on Pt/SiO_2 at 660 K and on Fe_3O_4/SiO_2 at 670 K when water vapor was present. Huber et al. [19] attributed the loss of H_2 chemisorption capacity and BET surface area of Co/SiO_2 catalyst during Fischer–Tropsch at 220 °C (493 K) to silica migration and formation of cobalt-silicates.

Lund and Dumesic [16] explained the migration of silica on Fe_3O_4 by Si^{4+} substitution into the tetrahedral sites of Fe_3O_4 and displacement of Fe^{3+} to adjacent octahedral sites, which occurred over the entire surface of Fe_3O_4, rather than being confined to the interface. The substituted Fe_3O_4 retained 80% capacity to adsorb NO but showed one order of magnitude lower turnover rate for water–gas shift reactions because there were still octahedrally coordinated iron cations on the surface that could adsorb NO but this compound was not active for catalytic reaction. A similar explanation may be applicable to the Pd system. Another possibility for silica migration is that silica interacted with water to form a mobile compound that migrated to the palladium particle surface.

Silica migration was also observed by TEM on the supported Pd/SiO_2 samples after reduction and after reaction. Similar migration of titania on rhodium during reduction has been seen after high-temperature reduction [49], and is believed to be the explanation for the phenomenon of strong metal–support interaction. If the surface overlayers were caused by Pd oxide, they would not be amorphous since PdO is generally crystalline (Figs. 2, 3, and 7). Hydrogen reduction of silica-supported palladium catalysts can also lead to strong chemical interaction between metal and

support and the growth of palladium silicides [10–12]. If we use the rate per gram of Pd as an indication of the surface area of Pd available during reaction (Table 1), it can be concluded that silica coverage must be higher on the sample reduced in H_2 than on the sample oxidized in O_2 since the rate is 45 times lower on the former sample. The TEM results confirm the higher concentration of silica on the reduced sample; the amorphous layer is clearly visible on the reduced sample but is diffuse on the oxidized sample after reaction. Juszczyk and Karpinski [11] proposed that overlayers of oxidized silicon species on palladium were formed only when the catalyst was first reduced at high temperature and then oxidized. During reduction, palladium silicides (Pd_xSi_y) were formed by palladium atoms taking oxygen vacancies in the silica support. When exposed to O_2 at room temperature, silicon in Pd_xSi_y was oxidized and then moved to the top of the surface; at the same time palladium atoms agglomerated and formed palladium particles, which were covered by silica.

4.2. Pd surface area and rates of reaction

The effects of oxidation and reduction on the surface area and reactivity of palladium catalysts has been studied [50]. In our work (Table 1), the higher surface area for the oxidized catalysts was caused probably by palladium surface roughening during O_2 oxidation, although the TEM pictures presented here do not suggest a substantial difference in surface roughening between reduced and oxidized samples. Ruckenstein and Chen [51] suggested that a particle breakup, not observed by TEM in our experiments either, could be the explanation for higher surface area. Datye [24] suggested based on TEM results that the surface of Rh catalysts was roughened when the sample was oxidized in O_2 and then reduced in H_2 at a mild temperature. The roughening is caused by an expansion of the metal structure upon oxidation, a situation similar to the one we have here. Results from our group on a Pd foil [28] show that the surface area of PdO increases by a factor of two after the combustion reaction. The increase in surface area by a factor of 1.5 for Pd/ZrO_2 after oxidation observed in our work is thus reasonable. Note also that for the samples supported on zirconia, the surface increase corresponded to a proportional increase in the rate per gram so that the turnover rate was constant. For the samples supported on silica, the decline in the chemisorption uptake by a factor of three after reduction seems to be affected by the coverage of Pd by silica. The decrease in chemisorptive properties (factor of 3) is much smaller than the decrease observed in the rate per gram (factor of 45) (Table 1). One explanation for this difference is that the overlayers of oxidized silicon formed during H_2 reduction might have moved during the surface area measurement by the H_2–O_2 titration procedure, causing a higher coverage. This is a feasible mechanism as the titration involves oxidation and reduction steps at 373 K. In this case, more active sites could be counted by H_2–O_2 titration than could be available during reaction of methane oxidation. This overcounting translates into a lower turnover rate than the correct one and would explain why the turnover rate of reduced Pd/SiO_2 was 1/15 of that for oxidized Pd/SiO_2 after 24 h on stream.

The rates of reaction for the foil and supported sample were in good agreement with the rates reported in the literature (Table 1). The general behavior of activation and deactivation are also the same as reported in the literature. For example, the zero rate of reaction at time zero for the prereduced samples observed in Figs. 5 and 6 has been observed before [52,53]. In this study, activation followed by deactivation was observed on Pd/ZrO_2 samples. Literature results suggest, for example, that during the activation stage new surface morphologies that are more active in oxidizing methane are formed and that palladium oxide particles sinter during the deactivation stage [17,18,31,54–57]. There was only deactivation observed on oxidized Pd/SiO_2, which was different from the other three catalysts tested and can probably be explained by silica migration. For oxidized Pd/SiO_2, silica started to spread once water was formed at the start of reaction. The initial activation caused possibly by a surface morphology change of PdO particle overlapped with deactivation by silica migration. The magnitude of deactivation was larger than the magnitude of activation, so deactivation, not activation, was observed at the first stage. Experimental results from Muto et al. [17,18] showed that in Pd/SiO_2 and Pd/SiO_2–Al_2O_3 samples with enough silica loading to cover the surface, only the deactivation stage was observed, which is in agreement with our results.

5. Conclusion

Silica from the support could migrate on to palladium particles during H_2 reduction or methane oxidation and also spread from silicon impurities present on the foil during methane oxidation. Migration during reaction was caused by water formed in the reaction, and migration during H_2 reduction of silica-supported catalyst was possibly caused by the formation of palladium silicides, subsequently oxidized by O_2. The migration of silica deactivated the catalyst by covering active sites. We conclude that silica is not a good support for Pd catalysts when they are used in reactions where water is present and also that they should not be reduced in H_2 at temperatures close to 900 K. These results explain the deactivation observed in this work on foils during methane oxidation. It points to possible problems when Pd massive catalysts (foil and wires) are used in reaction media containing water and H_2. When bulk Pd is used, surface science techniques need to be available to measure the state of the surface. When Pd is supported on zirconia, no deleterious effects caused by H_2 or H_2O are observed.

Acknowledgments

We gratefully acknowledge support from the Office of Basic Energy Sciences, Chemical Sciences, U.S. Department of Energy, Grant DE-FG02-00ER15408.

References

[1] J.G. McCarty, M. Gusman, D.M. Lowe, D.L. Hildenbrand, K.N. Lau, Catal. Today 47 (1999) 5.
[2] M. Haruta, S. Tsubota, T. Kobayashi, H. Kageyama, M.J. Genet, B. Delmon, J. Catal. 144 (1993) 175.
[3] S.J. Tauster, S.C. Fung, R.L. Garten, J. Am. Chem. Soc. 100 (1978) 170.
[4] S.J. Tauster, S.C. Fung, R.T.K. Baker, J.A. Horsley, Science 211 (1981) 1121.
[5] G.L. Haller, D.E. Resasco, Adv. Catal. 36 (1989) 173.
[6] S.J. Tauster, Acc. Chem. Res. 20 (1987) 389.
[7] A.T. Bell, in: L.L. Hegedus (Ed.), Catalyst Design: Progress and Perspectives, Wiley, New York, 1987.
[8] R. Burch, Chem. Ind. 31 (1988) 347.
[9] M.A. Vannice, Catal. Today 12 (1992) 255.
[10] R. Lamber, N. Laeger, G. Schulz-Ekloff, J. Catal. 123 (1990) 285.
[11] W. Juszczyk, Z. Karpinski, J. Catal. 117 (1989) 519.
[12] W. Juszczyk, D. Lomot, J. Pielaszek, Z. Karpinski, Catal. Lett. 78 (2002) 95.
[13] P.A. Crozier, R. Sharma, A.K. Datye, Microsc. Microanal. 4 (1998) 278.
[14] C.R.F. Lund, J.A. Dumesic, J. Catal. 72 (1981) 21.
[15] C.R.F. Lund, J.A. Dumesic, J. Catal. 76 (1982) 93.
[16] C.R.F. Lund, J.A. Dumesic, J. Phys. Chem. 86 (1982) 130.
[17] K.-I. Muto, N. Katada, M. Niwa, Appl. Catal. A 134 (1996) 203.
[18] K.-I. Muto, N. Katada, M. Niwa, Catal. Today 35 (1997) 145.
[19] G.W. Huber, C.G. Guymon, T.L. Conrad, B.C. Stephenson, C.H. Bartholomew, Stud. Surf. Sci. Catal. 139 (2001) 423.
[20] R.L. Moss, D. Pope, B.J. Davis, D.H. Edwards, J. Catal. 58 (1979) 206.
[21] W. Juszczyk, Z. Karpinski, D. Lomot, J. Pielaszek, J. Catal. 220 (2003) 299.
[22] B.K. Min, A.K. Santra, D.W. Goodman, Catal. Today 85 (2003) 113.
[23] D. Wang, S. Penner, D.S. Su, G. Rupprechter, K. Hayek, R. Schlögl, J. Catal. 219 (2003) 434.
[24] A.K. Datye, Top. Catal. 13 (2000) 131.
[25] W. Stoeber, A. Fink, E. Bohn, J. Colloid Interface Sci. 26 (1968) 62.
[26] J.E. Benson, H.S. Hwang, M. Boudart, J. Catal. 30 (1973) 146.
[27] J.R. Anderson, in: Structure of Metallic Catalysts, Academic Press, New York, 1975, p. 296.
[28] R.S. Monteiro, D. Zemlyanov, J.M. Storey, F.H. Ribeiro, J. Catal. 199 (2001) 291.
[29] C.D. Wagner, L.E. Davis, M.V. Zeller, J.A. Taylor, R.H. Raymond, L.H. Gale, SIA, Surf. Interface Anal. 3 (1981) 211.
[30] F.H. Ribeiro, M. Chow, R.A.D. Betta, J. Catal. 146 (1994) 537.
[31] K. Fujimoto, F.H. Ribeiro, M. Avalos-Borja, E. Iglesia, J. Catal. 179 (1998) 431.
[32] R. Baptist, A. Pellissier, G. Chauvet, Solid State Commun. 68 (1988) 555.
[33] T. Ogama, J. Appl. Phys. 64 (1988) 753.
[34] E. Puppin, I.I.A. Lindau, Solid State Commun. 77 (1991) 983.
[35] E. Gorlich, J. Haber, A. Stoch, J. Stoch, J. Solid State Chem. 33 (1980) 121.
[36] H. Seyama, M. Soma, J. Chem. Soc., Faraday Trans. I 81 (1985) 485.
[37] M. Anpo, H. Nakaya, S. Kodama, Y. Kubokawa, K. Domen, T. Onishi, J. Phys. Chem. 90 (1986) 1633.
[38] E. Paparazzo, J. Phys. D 20 (1987) 1091.
[39] S.D. Bader, L. Richter, T.W. Orent, Surf. Sci. 115 (1982) 501.
[40] G.V. Samsonov (Ed.), The Oxide Handbook, IFI/Plenum, New York, 1973.
[41] T. Bekkay, E. Sacher, A. Yelon, Surf. Sci. 217 (1989) L377.
[42] S.W. Gaarenstroom, N. Winograd, J. Chem. Phys. 67 (1977) 3500.
[43] M. Bowker, Surf. Sci. 155 (1985) L276.
[44] L.H. Tjeng, M.B.J. Meinders, J. van Elp, J. Ghijsen, G.A. Sawatzky, R.L. Johnson, Phys. Rev. 41 (1990) 3190.
[45] D.Y. Zemlyanov, A. Nagy, R. Schlögl, Appl. Surf. Sci. 133 (1998) 171.
[46] R. Behrisch, in: Sputtering by Particle Bombardment I: Physical Sputtering of Single-Element Solids, Springer-Verlag, Berlin, 1981.
[47] M.P. Seah, SIA, Surf. Interface Anal. 2 (1980) 222.
[48] C.J. Powell, A. Jablonski, in: NIST Electron Inelastic-Mean-Free-Path Database, National Institute of Standards and Technology, Gaithersburg, 2000.
[49] A.D. Logan, E.J. Braunschweig, A.K. Datye, D.J. Smith, Langmuir 4 (1988) 827.
[50] D. Ciuparu, M.R. Lyubovsky, E. Altman, L.D. Pfefferle, A. Datye, Catal. Rev.-Sci. Eng. 44 (2002) 593.
[51] E. Ruckenstein, J.J. Chen, J. Colloid Interface Sci. 86 (1982) 1.
[52] R. Burch, F.J. Urbano, Appl. Catal. A 124 (1995) 121.
[53] R. Burch, P.K. Loader, F.J. Urbano, Catal. Today 27 (1996) 243.
[54] E. Garbowski, C. Feumi-Jantou, N. Mouaddib, M. Primet, Appl. Catal. A 109 (1994) 277.
[55] E. Garbowski, C. Feumi-Jantou, N. Mouaddib, M. Primet, Appl. Catal. A 125 (1995) 185.
[56] T.R. Baldwin, R. Burch, Appl. Catal. 66 (1990) 359.
[57] T.R. Baldwin, R. Burch, Catal. Lett. 6 (1990) 131.